



Cite this: *Org. Biomol. Chem.*, 2023, **21**, 1942

Received 1st December 2022,
Accepted 17th January 2023
DOI: 10.1039/d2ob02193e
rsc.li/obc

Diyne-steered switchable regioselectivity in cobalt(II)-catalysed C(sp²)-H activation of amides with unsymmetrical 1,3-diyne[†]

Prakriti Dhillon, Prasad Anaspure, Jesper G. Wiklander, Subban Kathiravan and Ian A. Nicholls *

The regiochemical outcome of a cobalt(II) catalysed C–H activation reaction of aminoquinoline benzamides with unsymmetrical 1,3-diyne under relatively mild reaction conditions can be steered through the choice of diyne. The choice of diyne provides access to either 3- or 4-hydroxyalkyl isoquinolinones, paving the way for the synthesis of more highly elaborate isoquinolines.

Introduction

Transition metal catalysed C–H bond activation is an important method for the synthesis of a broad range of bioactive molecules and materials without the need for prefunctionalisation, thus minimising waste and enhancing atom economy.^{1–5} Traditionally, despite their low abundance and toxicity, transition metals such as palladium,⁶ rhodium,^{7–9} ruthenium,^{10–12} and iridium¹³ have been the catalysts of choice for efficient C–H bond activation.¹⁴ However, the past decade has witnessed a shift towards more abundant and comparatively less toxic base metal catalysts.¹⁴ In this context, cobalt has been of significant interest due to its high relative abundance and the unique catalytic activities provided by this element's three oxidation states.^{15–18} Very recently, Niu and co-workers developed a Co(II)/organic oxidant catalytic system for the selective activation of 1°, 2°, and 3° C-(sp³)-H bonds for constructing C–N and C–O bonds.¹⁹ Knochel and co-workers synthesised organozinc pivalates using cobalt-catalysed cross-coupling reactions.²⁰ Numerous elegant examples of cobalt-catalysed C–H activations have been reported by Daugulis,^{21–23} Glorius,^{24–27} Ackermann,^{26,27} and others.^{28–30}

Although cobalt catalysts have made available a variety of new disconnections, the regioselective synthesis of heterocycles using an unsymmetrical coupling partner remains unrealised. In addition, the basis for regiochemical preferences associated with 1,3-diyne-based annulations has not yet been investigated.

Many isoquinolones are highly bioactive molecules and their synthesis through C–H activation has been realised with various alkynes.^{31–34} C–H activation strategies employing 1,3-diyne addition have become important methods to synthesise this important heterocyclic moiety. For example, Miura first achieved the synthesis of isoquinolones by C–H activation using Rh(III) catalysts.³⁵ Glorius developed a novel route for the synthesis of conjugated isoquinolones and bis-heterocycles through double C–H activation.³⁶ Later, we developed a cobalt catalysed C–H activation of benzamides with 1,3-diyne using aminoquinoline as a chelating group (Fig. 1a).³⁷ After these initial developments, research teams have disclosed a range of interesting examples with symmetrical 1,3-diyne (Scheme 1a).^{38–42} Nonetheless, the use of unsymmetrical 1,3-diyne has been limited. This may be due to the inherent possibility of metalloalkynylation through two similar sites, leading to several possible regioisomers (Fig. 1b). For example, Jeganmohan and co-workers have reported that four different unsymmetrical 1,3-diyne when used in a cobalt(III) catalysed regioselective (4 + 2) annulation of sulfoxonium ylides provided two regioisomeric products.^{43,45} A Rh(III) catalysed (3 + 2) spirocyclisation of 2H-imidazoles with unsymmetrical 1,3-diyne was also reported by the Dong group.⁴⁴ In this case, the regioselectivity was comparable to that of our cobalt system.³⁷ Given the potential regiochemical promiscuity available when using unsymmetrical 1,3-diyne, we envisaged that the nature of the 1,3-diyne could have an impact on the preferred outcome of the reaction. Herein, we report our findings on the cobalt(II) catalysed C–H activation of aminoquinoline benzamides with unsymmetrical 1,3-diyne (Fig. 1c).

Bioorganic & Biophysical Chemistry Laboratory, Linnaeus University Centre for Biomaterials Chemistry, Department of Chemistry & Biomedical Sciences, Linnaeus University, Kalmar SE-39182, Sweden. E-mail: ian.nicholls@lnu.se

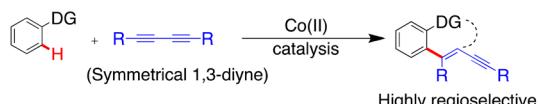
† Electronic supplementary information (ESI) available: Experimental details, copies of NMR spectra, HRMS spectra and XRD-data. CCDC 2041954, 2041960, 2041961, 2041962, 2041992 and 2042374. For ESI and crystallographic data in CIF or other electronic format see DOI: <https://doi.org/10.1039/d2ob02193e>

Results and discussion

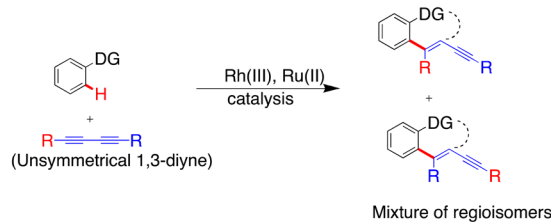
Reactions were performed using 2.0 equiv. of benzamide (**1a–g**) and 1.0 equiv. of unsymmetrical 1,3-diyne (**2–5**) as the



a) Our previous work



b) Recent examples with unsymmetrical 1,3-dynes



c) This work with unsymmetrical 1,3-dynes

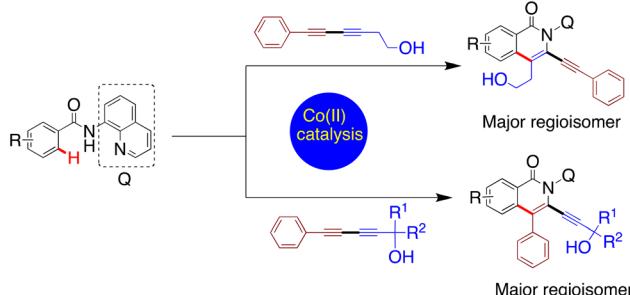
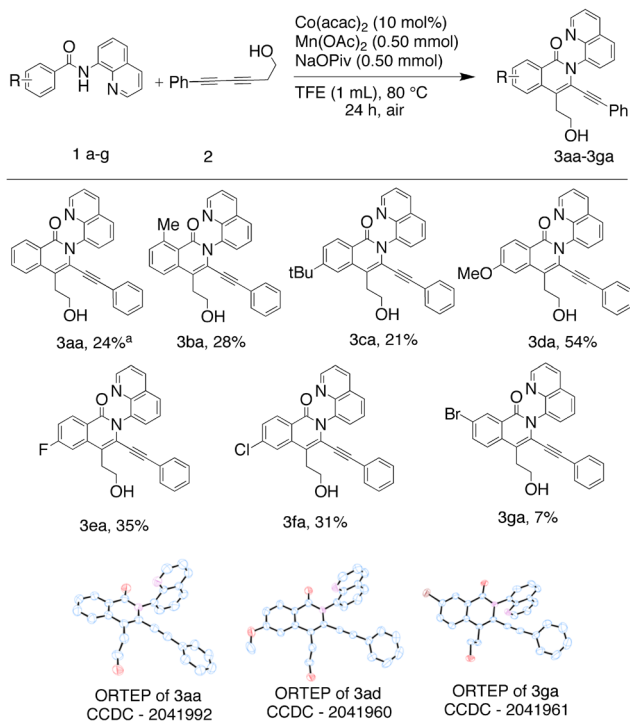


Fig. 1 Regioselective C–H activation.

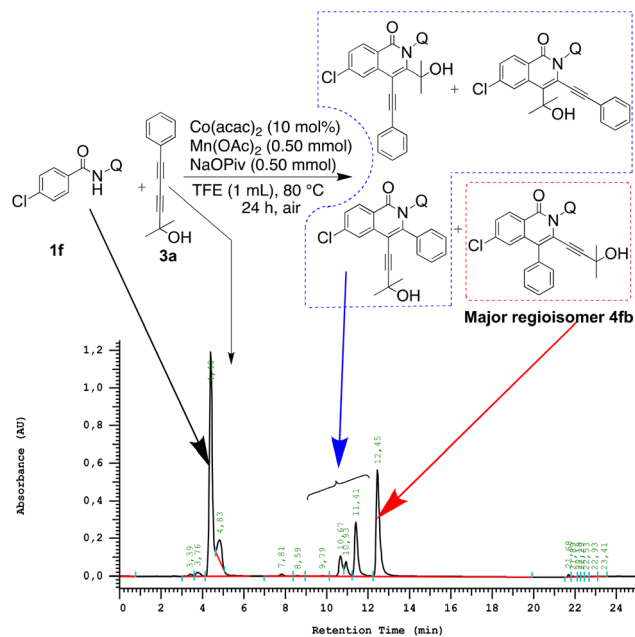
Scheme 1 Substrate scope with 1,3-diyne 2 (³*in situ* yields were calculated by HPLC).

starting substrates for the C–H annulation reaction using 10 mol% of cobalt(II)acetylacetone, 2.0 equiv. of manganese (II)acetate as the external oxidant, 2.0 equiv. of sodium tri-

methylacetate hydrate as the base and 2,2,2-trifluoroethanol (TFE) as the solvent. These conditions were selected to provide moderate yields of the major regioisomer, so that the eventual influence on yields due to variations in the amides and diynes used could be observed.

In the case of unsubstituted and *o*- and *p*-substituted amides, four modes of insertions are possible, leading to four possible regioisomeric isoquinolone products and eight possible products when the amide bears an *m*-substituent. The reactions were carried out under air, at 80 °C for 24 h. In each case, the major regioisomer was isolated and purified by flash column or preparative thin layer chromatography and 2D NMR elucidated structures. 2D NMR data were further confirmed by XRD, where possible. An HPLC-assay was developed and used to determine the *in situ* yields of the major regioisomers from each of the C–H activation reactions, *i.e.* the yield as determined from the reaction vessel prior to work-up and purification. The HPLC-assay also revealed the presence of unreacted starting materials and minor isomers, and the latter, in some cases, could be isolated and characterized (Fig. 2).

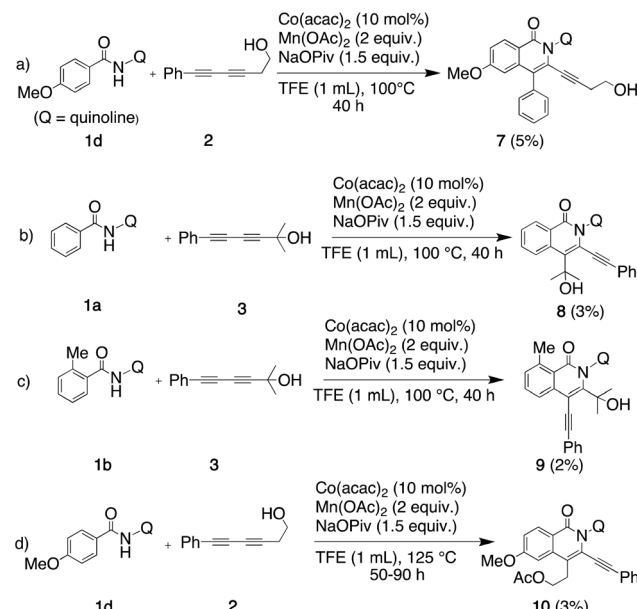
Initial efforts employed a series of benzamides (**1a–g**) and an unsymmetrical diyne (**2**) with a polar hydroxyl functionality and less steric bulk than in the apolar symmetrical diynes used in previous studies. The corresponding products displayed the same preferred geometry of insertion of the unsymmetrical diyne as that reported in our earlier work using symmetrical 1,3-dynes,³⁷ namely with the resulting phenyl bearing alkynyl substituent *ortho* to the isoquinolone nitrogen (Scheme 1), with the hydroxyalkyl bearing alkyne being the preferred insertion partner. The reaction was generally tolerant

Fig. 2 HPLC trace of the crude reaction mixture of **1f** with **3**, with unreacted starting materials, isolated major regioisomer and peaks arising from the expected non-isolated minor regioisomers marked.

toward a range of benzamide substituents. Of note was the significantly better yield associated with the strongly electron donating *p*-methoxy (3da), relative to the unsubstituted case (3aa), and the low yield of the major regioisomer from the reaction performed using *m*-bromobenzamide (1g), where the low yield was attributed to a combination of the competition between eight insertion modes and the steric hindrance afforded by the bromo-substituent.

We then deployed an isopropyl alcohol-substituted diyne (3), a slightly bulkier and shorter diyne (containing one additional carbon and a quaternary carbon, as compared to 2), with the same series of benzamides (1a–g) (Scheme 2). Again, all the major regioisomers displayed the alkynyl substituent *ortho* to the isoquinolone nitrogen; however, and to our surprise, the orientation of insertion in all major products was reversed with respect to the orientation of the diyne-substituents obtained when using 2. Moreover, the yield of the unsubstituted benzamide product was notably higher compared to its reaction with diyne 2. Again, the strongly electron-donating *p*-methoxy substituent produced the highest yield, and even the yield of the reaction with *m*-bromobenzamide improved. The reactivity of two substantially more sterically demanding diynes (4 and 5) was then explored, with the major regioisomers again demonstrating the reversal of orientation of insertion, though with lower yields, possibly reflecting the impact of the increased bulk of the branched hydroxyl bearing substituents on the reaction energetics of metallocycle formation.

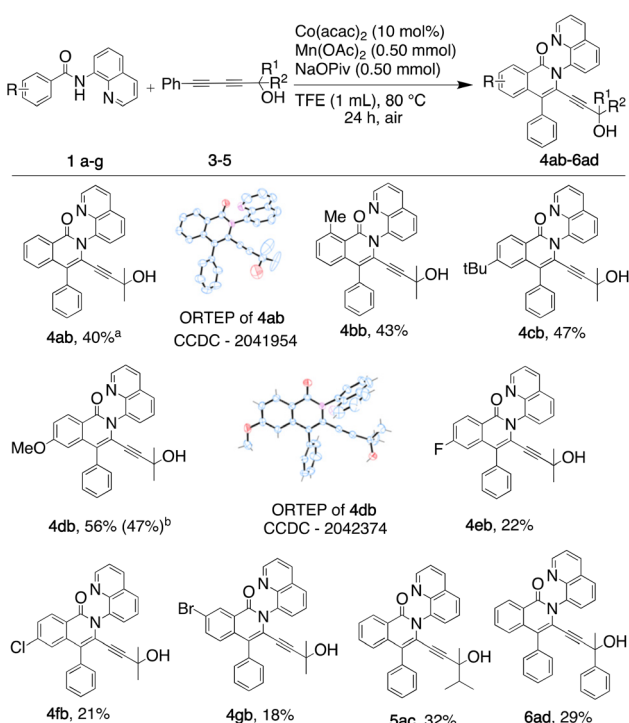
When some reactions were performed using longer reaction times and higher temperatures (Scheme 3), the regiochemis-



Scheme 3 Isolated minor regioisomers and acetylated by-products (isolated yields).

tries of the dominant regioisomers and their yields remained essentially the same, although the yields of three of the minor isomers increased to levels that permitted isolation and structural determination by 2D-NMR (7–9, Scheme 3a–c). Harsher conditions also led to the isolation of an acetylated by-product in some cases using the least sterically hindered diyne (2) (10, Scheme 3d).

Our rationalisation of the observed regioselectivity is based on our previous report³⁹ and literature precedent.^{40–46} In our earlier work using symmetrical bulky diphenyl- and diphenoxyl-1,3-diyne, the major regioisomers obtained each had the alkynyl substituent at the 3-position, *ortho* to the amide nitrogen and its pendent quinolinyl directing group. The steric bulk of the directing group makes the approach of the diyne for metallocycle formation easier with the bulky substituent furthest from the quinolinyl moiety. The same preference for insertion was observed for all reactions with the unsymmetrical diynes used in the present study, although with a substituent-dependent switch in the preferred orientation of insertion. The unsymmetrical diynes used had a bulky non-polar phenyl substituent and a hydroxyl-bearing alkyl chain. The switch was observed between reactions performed using the least sterically hindered hydroxyl diyne (2) and the diynes with more sterically demanding hydroxyl-bearing substituents (Fig. 3). We propose that the orientation of insertion of diyne 2 could be steered by the hydroxyl through a secondary interaction with the metal centre influencing the migratory insertion or its coordination to the metal centre and interaction, which is not feasible when the bulkier diynes are employed. Thus, the cobalt complex A reacts with diarynes 2 and 3 to give complexes B and E with two diyne orientations possible for coordination. There is a selection of one cobalt-diyne complex (C and F)



Scheme 2 Substrate scope with 1,3-diyne 3–5. ^a*in situ* yields were calculated by HPLC. ^bisolated yield.



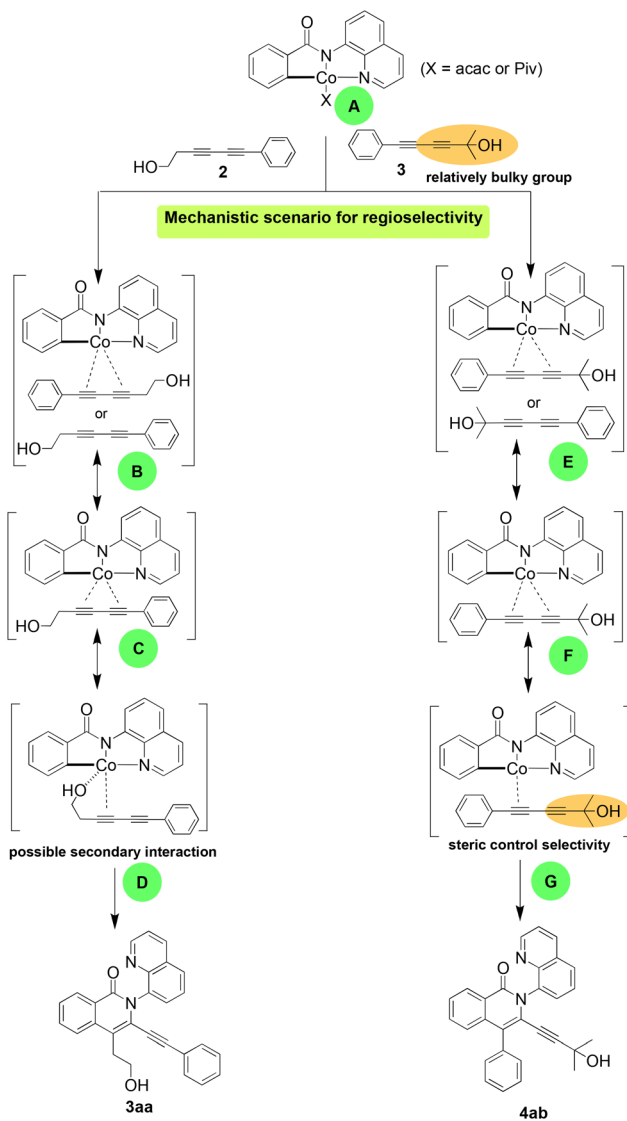
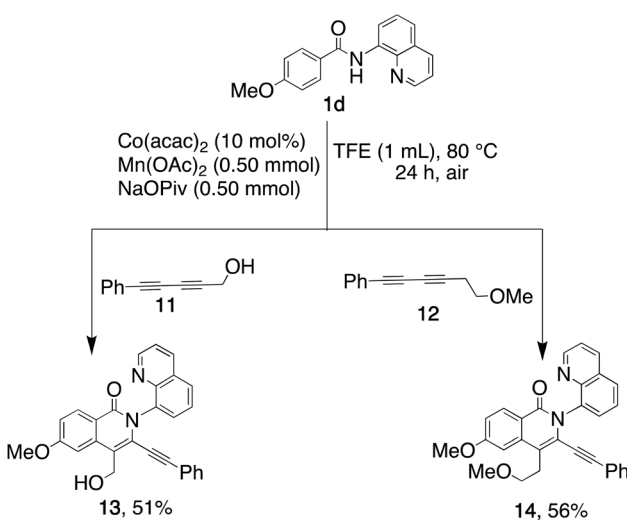


Fig. 3 Proposed mechanistic scenario for the observed regioselectivity.



Scheme 4 Mechanistic studies with diynes 11 and 12.

leading to **D** and **G**, and their corresponding products (**3aa** and **4ab**) as the major regioisomers.

To test this hypothesis, we expanded our mechanistic studies to include diyne **11**, with less bulk than diyne **2**, and diyne **12**. Importantly, the regioselectivity observed with **2** was maintained, resulting in the formation of the corresponding products **13** (51%) and **14** (56%) (Scheme 4). The less sterically hindered diynes thus appear to coordinate with the cobaltocycle through the substituent oxygen, facilitating the preferred regioselectivity.

Conclusions

In summary, we report a regioselective cobalt catalysed C–H activation reaction of aminoquinoline benzamides with unsymmetrical 1,3-dynes that can be performed under relatively mild conditions. This reaction furnishes the corresponding 3- or 4-hydroxyalkyl substituted heterocycles with the regiochemistry of the dominant product determined by the nature of the substituents present on the 1,3-dyne. The ability to predetermine the orientation of insertion and subsequent location of functionality should be a valuable tool for the synthesis of isoquinolinone-derived materials or bioactive agents.

Experimental details

General procedure for cobalt catalyzed C–H activation with unsymmetrical diynes (Schemes 1 & 2)

In an oven dried reaction tube, charged with a magnetic stir-bar, unsymmetrical 1,3-dyne (0.25 mmol, 1.0 equiv.), Co(acac)₂ (10 mol%), benzamide (0.50 mmol, 2.0 equiv.), Mn(OAc)₂ (0.50 mmol, 2.0 equiv.), and NaOPiv (0.50 mmol, 2.0 equiv.) were added. Then, TFE (1 mL) was added to the system and the reaction was stirred at 80 °C for 24 h. The major regioisomer was isolated through flash chromatography in petroleum ether : acetone (3 : 2) and characterized by NMR, IR and HRMS.

General procedure for control experiments (Scheme 3)

In an oven dried reaction tube, charged with a magnetic stir-bar, unsymmetrical 1,3-dyne (0.58 mmol, 1.0 equiv.), Co(acac)₂ (10 mol%), benzamide (0.86 mmol, 1.5 equiv.), Mn(OAc)₂ (1.15 mmol, 2.0 equiv.), and NaOPiv (0.87 mmol, 1.5 equiv.) were added. Then, TFE (1 mL) was added to the system and the reaction was stirred at 100–125 °C for 40–90 h. The major and minor regioisomer and the acylated by-products were isolated through flash chromatography and preparative TLC in petroleum ether : acetone (3 : 2) and characterized by NMR, IR and HRMS.

HPLC-based yield determination

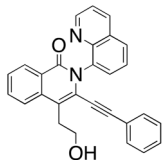
As the reaction resulted in complex mixtures due to the presence of minor isomers with similar chromatographic properties, an HPLC-based assay was proposed as a tool to directly determine the yield of the major isomer *in situ*, to avoid misin-



terpretation of reaction outcomes due to losses during purification. From the reaction mixture, 15 μ L sample was taken and made up to 1 mL in 2-propanol with a dilution factor of 66.66. Pure samples of each of the major regiosomeric products with a stock solution of 3 mg mL^{-1} were used to construct calibration curves. The chromatograms were recorded using a D-7000 HSM software on a gradient method (petroleum ether/2-propanol) with a flow rate of 1 mL min^{-1} , injection volume 10 μL , and acquisition wavelength ranging from 280–330 nm.

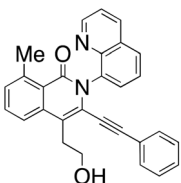
Experimental data

4-(2-Hydroxyethyl)-3-(2-phenylethynyl)-2-(quinolin-8-yl)-1,2-dihydroisoquinolin-1-one (3aa).



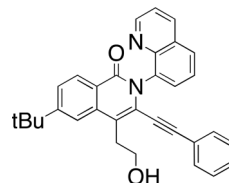
M.P.: 149–150 $^{\circ}\text{C}$; **Appearance:** brown crystal; **HPLC yield:** 24%; **$^1\text{H NMR}$ (400 MHz, Methanol- d_4 , δ 3.31)** δ 8.80 (dd, J = 4.3, 1.7 Hz, 1H), 8.52 (dd, J = 8.4, 1.7 Hz, 1H), 8.44 (ddd, J = 8.0, 1.4, 0.6 Hz, 1H), 8.20 (dd, J = 8.2, 1.5 Hz, 1H), 8.05 (ddd, J = 8.3, 1.1, 0.6 Hz, 1H), 7.94–7.85 (m, 2H), 7.83 (dd, J = 8.2, 7.3 Hz, 1H), 7.65 (ddd, J = 8.1, 7.1, 1.1 Hz, 1H), 7.59 (dd, J = 8.3, 4.3 Hz, 1H), 7.27–7.19 (m, 1H), 7.18–7.09 (m, 2H), 6.71–6.65 (m, 2H), 3.96–3.88 (m, 2H), 3.40 (dd, J = 7.7, 6.8 Hz, 2H). **$^{13}\text{C NMR}$ (101 MHz, Methanol- d_4 , δ 49.00)** δ 164.0, 152.1, 145.5, 138.7, 138.5, 138.1, 134.4, 131.9, 131.9, 130.9, 130.8, 130.2, 129.3, 129.2, 128.9, 127.8, 127.6, 126.9, 125.3, 123.2, 122.4, 120.8, 100.9, 83.6, 62.3, 33.7. **FTIR (cm⁻¹)**: 3412, 2140, 1651, 1599, 1328, 1033, 740. **HRMS** $\text{C}_{28}\text{H}_{20}\text{N}_2\text{O}_2$ [M + H $^+$]: calculated: 473.2229, found: 473.2228.

4-(2-Hydroxyethyl)-6-methoxy-3-(2-phenylethynyl)-2-(quinolin-8-yl)-1,2-dihydroisoquinolin-1-one (3da).



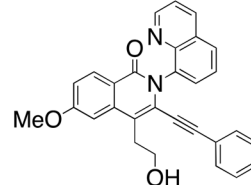
M.P.: 188–190 $^{\circ}\text{C}$; **Appearance:** brown crystal; **HPLC yield:** 28%; **$^1\text{H NMR}$ (400 MHz, DMSO- d_6 , δ 2.50)** δ 8.84 (dd, J = 4.2, 1.7 Hz, 1H), 8.52 (dd, J = 8.4, 1.7 Hz, 1H), 8.32–8.10 (m, 1H), 7.91–7.87 (m, 1H), 7.84 (d, J = 8.3 Hz, 1H), 7.80 (t, J = 7.7 Hz, 1H), 7.73 (t, J = 7.7 Hz, 1H), 7.58 (dd, J = 8.3, 4.2 Hz, 1H), 7.39 (d, J = 7.4 Hz, 1H), 7.27 (d, J = 7.3 Hz, 1H), 7.21 (t, J = 7.3 Hz, 2H), 6.74–6.57 (m, 2H), 4.90 (s, 1H), 3.69 (t, J = 7.5 Hz, 2H), 3.22 (t, J = 7.5 Hz, 2H), 2.76 (s, 3H). **$^{13}\text{C NMR}$ (101 MHz, DMSO- d_6 , δ 39.52)** δ 161.6, 150.9, 144.2, 141.5, 138.0, 137.8, 136.3, 132.2, 130.8, 130.5, 130.3, 129.2, 128.9, 128.7, 128.6, 126.3, 125.3, 124.5, 122.4, 121.9, 120.7, 117.7, 98.3, 83.1, 60.5, 33.3, 23.8. **FTIR (cm⁻¹)**: 3244.24, 3057.93, 2115.84, 1653, 1555.67, 1359.58, 1031.15, 750.40. **HRMS** $\text{C}_{29}\text{H}_{22}\text{N}_2\text{O}_2$ [M + H $^+$]: calculated: 431.1760, found: 431.1755.

6-*tert*-Butyl-4-(2-hydroxyethyl)-3-(2-phenylethynyl)-2-(quinolin-8-yl)-1,2-dihydroisoquinolin-1-one (3ca).



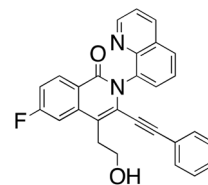
M.P.: 145–146 $^{\circ}\text{C}$; **Appearance:** off-white crystal; **HPLC yield:** 21%; **$^1\text{H NMR}$ (400 MHz, DMSO- d_6 , δ 8.81)** δ 8.81 (dd, J = 4.2, 1.7 Hz, 1H), 8.53 (dd, J = 8.4, 1.7 Hz, 1H), 8.23 (d, J = 5.5 Hz, 1H), 8.22–8.19 (m, 1H), 7.92 (d, J = 1.8 Hz, 1H), 7.91 (dd, J = 7.4, 1.5 Hz, 1H), 7.81 (t, J = 7.8 Hz, 1H), 7.72 (dd, J = 8.5, 1.8 Hz, 1H), 7.58 (dd, J = 8.3, 4.2 Hz, 1H), 7.31–7.25 (m, 1H), 7.22 (dd, J = 8.2, 6.5 Hz, 2H), 6.72–6.62 (m, 2H), 4.95 (t, J = 5.7 Hz, 1H), 3.73 (q, J = 6.9 Hz, 2H), 3.26 (dt, J = 7.3, 4.6 Hz, 2H), 1.43 (s, 9H). **$^{13}\text{C NMR}$ (101 MHz, DMSO- d_6 , δ 160.6, 155.8, 151.0, 144.1, 137.6, 136.3, 136.0, 130.5, 130.3, 129.2, 129.1, 128.6, 128.6, 127.6, 126.2, 125.5, 125.3, 124.0, 121.9, 120.7, 120.2, 118.4, 98.4, 83.2, 60.7, 35.2, 32.9, 30.9. **FTIR (cm⁻¹)**: 2960.92, 1649.05, 1595.09, 1360.57, 1020.16, 784.554. **HRMS** $\text{C}_{32}\text{H}_{28}\text{N}_2\text{O}_2$ [M + H $^+$]: calculated: 473.2229, found: 473.2228.**

4-(2-Hydroxyethyl)-6-methoxy-3-(2-phenylethynyl)-2-(quinolin-8-yl)-1,2-dihydroisoquinolin-1-one (3da).



M.P.: 190–191 $^{\circ}\text{C}$; **Appearance:** white crystal; **HPLC yield:** 54%; **$^1\text{H NMR}$ (400 MHz, DMSO- d_6 , δ 2.50)** δ 8.83 (dd, J = 4.2, 1.7 Hz, 1H), 8.52 (dd, J = 8.3, 1.7 Hz, 1H), 8.24–8.17 (m, 2H), 7.90 (d, J = 7.2 Hz, 1H), 7.80 (t, J = 7.7 Hz, 1H), 7.58 (dd, J = 8.3, 4.2 Hz, 1H), 7.36 (d, J = 2.4 Hz, 1H), 7.31–7.18 (m, 3H), 6.68–6.63 (m, 2H), 4.93 (t, J = 5.7 Hz, 1H), 3.98 (s, 3H), 3.71 (q, J = 6.8 Hz, 2H), 3.21 (t, J = 7.5 Hz, 2H). **$^{13}\text{C NMR}$ (101 MHz, DMSO- d_6 , δ 39.52)** δ 162.8, 160.5, 151.0, 144.2, 138.3, 137.7, 136.4, 130.6, 130.4, 130.0, 129.4, 129.2, 128.7, 128.6, 126.3, 125.9, 122.0, 120.7, 119.9, 117.9, 116.1, 106.4, 98.5, 83.2, 60.6, 55.7, 33.0. **FTIR (cm⁻¹)**: 3370, 2963, 2175, 1599, 1567, 1486, 1377, 1328, 1226.478. **HRMS** $\text{C}_{29}\text{H}_{22}\text{N}_2\text{O}_3$ [M + H $^+$]: calculated: 447.1709, found: 447.1699.

6-Fluoro-4-(2-hydroxyethyl)-3-(2-phenylethynyl)-2-(quinolin-8-yl)-1,2-dihydroisoquinolin-1-one (3ea).

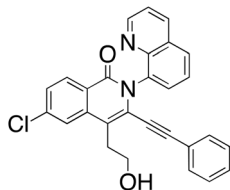


M.P.: 110–113 $^{\circ}\text{C}$; **Appearance:** off-white solid; **HPLC yield:** 35%; **$^1\text{H NMR}$ (400 MHz, CDCl $_3$, δ 7.26)** δ 8.85 (dd, J = 4.3,



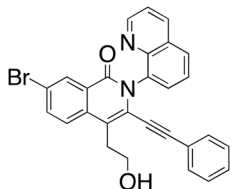
1.7 Hz, 1H), 8.53 (dd, J = 8.9, 6.0 Hz, 1H), 8.27 (dd, J = 8.4, 1.7 Hz, 1H), 8.01 (dd, J = 8.3, 1.4 Hz, 1H), 7.84 (dd, J = 7.3, 1.4 Hz, 1H), 7.72 (t, J = 7.8 Hz, 1H), 7.46 (dd, J = 10.4, 2.5 Hz, 1H), 7.41 (dd, J = 8.3, 4.2 Hz, 1H), 7.23 (m, 1H), 7.19 (m, 1H), 7.11 (dd, J = 8.3, 6.8 Hz, 2H), 6.67 (m, 2H), 3.94 (t, J = 6.8 Hz, 2H), 3.27 (t, J = 6.7 Hz, 2H). ^{13}C NMR (101 MHz, CDCl_3 , δ 77.16) δ 165.7 (d, J = 252.5 Hz), 161.5, 151.03, 139.3 (d, J = 9.9 Hz), 137.5, 136.6, 132.1 (d, J = 10.0 Hz), 131.0, 130.4, 129.2, 129.2, 129.0, 128.2, 127.3, 126.3, 123.3 (d, J = 2.0 Hz), 121.8, 121.3, 117.8 (d, J = 1.8 Hz), 115.8 (d, J = 23.3 Hz), 109.2 (d, J = 23.2 Hz), 100.0, 82.8, 61.9, 32.9. FTIR (cm^{-1}): 3436.60, 2921.91, 2111.50, 1639.35, 1606.65, 1486.42, 1369.79, 1044.82, 752.49. HRMS $\text{C}_{28}\text{H}_{19}\text{FN}_2\text{O}_2$ [M + H $^+$]: calculated: 435.1509, found: 435.1510.

6-Chloro-4-(2-hydroxyethyl)-3-(2-phenylethynyl)-2-(quinolin-8-yl)-1,2-dihydroisoquinolin-1-one (3fa).



M.P.: 166–168 °C; Appearance: light yellow solid; HPLC yield: 31%; ^1H NMR (400 MHz, CDCl_3 , TMS) δ 8.78 (d, J = 4.1 Hz, 1H), 8.38 (d, J = 8.6 Hz, 1H), 8.20 (d, J = 8.4 Hz, 1H), 7.94 (d, J = 8.2 Hz, 1H), 7.76 (d, J = 7.3 Hz, 1H), 7.75 (s, 1H), 7.65 (t, J = 7.8 Hz, 1H), 7.40 (d, J = 8.6 Hz, 1H), 7.35 (dd, J = 8.3, 4.2 Hz, 1H), 7.12 (t, J = 7.6 Hz, 1H), 7.04 (t, J = 7.7 Hz, 2H), 6.60 (d, J = 7.6 Hz, 2H), 3.90 (t, J = 6.8 Hz, 2H), 3.23 (t, J = 6.8 Hz, 2H). ^{13}C NMR (101 MHz, CDCl_3 , TMS) δ 160.5, 150.1, 143.4, 138.4, 137.1, 136.5, 135.4, 130.0, 129.6, 129.3, 128.2, 128.2, 128.0, 127.1, 126.8, 126.3, 125.3, 124.0, 122.3, 120.8, 120.2, 116.4, 99.1, 81.8, 60.9, 31.6. FTIR (cm^{-1}): 3057.93, 2959.50, 1647.49, 1594.43, 1326.38, 1024.06, 776.919. HRMS $\text{C}_{28}\text{H}_{19}\text{ClN}_2\text{O}_2$ [M + H $^+$]: calculated: 451.1213, found: 451.1207.

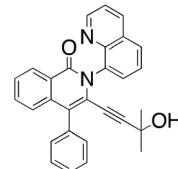
7-Bromo-4-(2-hydroxyethyl)-3-(2-phenylethynyl)-2-(quinolin-8-yl)-1,2-dihydroisoquinolin-1-one (3ga).



M.P.: 138–140 °C; Appearance: light yellow solid; HPLC yield: 7%; ^1H NMR (400 MHz, Methanol- d_4 , δ 3.31) δ 8.81 (dd, J = 4.3, 1.7 Hz, 1H), 8.53 (td, J = 4.6, 4.0, 1.7 Hz, 2H), 8.22 (dd, J = 8.2, 1.5 Hz, 1H), 8.01 (dd, J = 8.8, 2.1 Hz, 1H), 7.97 (d, J = 8.8 Hz, 1H), 7.91 (dd, J = 7.4, 1.5 Hz, 1H), 7.84 (dd, J = 8.2, 7.4 Hz, 1H), 7.61 (dd, J = 8.3, 4.3 Hz, 1H), 7.26–7.21 (m, 1H), 7.17–7.12 (m, 2H), 6.70–6.66 (m, 2H), 3.91 (t, J = 7.2 Hz, 2H), 3.37 (t, J = 7.1 Hz, 2H). ^{13}C NMR (101 MHz, Methanol- d_4 , δ 49.00) δ 162.8, 152.2, 145.4, 138.5, 138.4, 137.3, 137.1, 131.9, 131.8, 131.6, 131.0, 130.9, 130.4, 129.4, 129.0, 127.8, 127.5, 123.3, 122.6, 122.3, 120.4, 101.4, 83.4, 62.2, 33.7. FTIR (cm^{-1}):

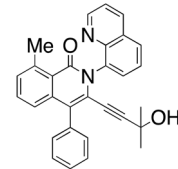
3402.42, 2955.98, 2203.72, 1634.24, 1567.45, 1476.06, 1324.90, 1047.19, 785.95. HRMS $\text{C}_{28}\text{H}_{19}\text{BrN}_2\text{O}_2$ [M + H $^+$]: calculated: 497.0688, found: 497.0688.

3-(3-Hydroxy-3-methylbut-1-yn-1-yl)-4-phenyl-2-(quinolin-8-yl)-1,2-dihydroisoquinolin-1-one (4ab).



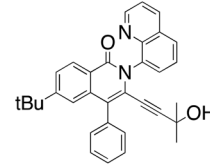
M.P.: 218–220 °C; Appearance: light brown crystal; HPLC yield: 40%; ^1H NMR (400 MHz, DMSO- d_6) δ 8.87 (dd, J = 4.2, 1.7 Hz, 1H), 8.50 (dd, J = 8.4, 1.7 Hz, 1H), 8.34–8.25 (m, 1H), 8.15 (dd, J = 8.3, 1.4 Hz, 1H), 7.88 (dd, J = 7.3, 1.4 Hz, 1H), 7.76 (ddd, J = 8.3, 7.3, 1.2 Hz, 2H), 7.66–7.55 (m, 2H), 7.55–7.39 (m, 5H), 7.31 (dt, J = 8.0, 1.0 Hz, 1H), 4.77 (s, 1H), 0.54 (s, 3H), 0.51 (s, 3H). ^{13}C NMR (101 MHz, DMSO- d_6) δ 160.9, 150.8, 144.1, 137.3, 136.4, 136., 135.3, 132.9, 130.9, 130.8, 130.1, 129.0, 128.7, 128.3, 127.8, 127.6, 126.1, 125.7, 125.2, 125.2, 122.3, 121.8, 105.1, 75.0, 62.8, 30.0. FTIR (cm^{-1}): 3068, 2973, 2145, 1627, 1497, 1578. HRMS $\text{C}_{29}\text{H}_{22}\text{N}_2\text{O}_2$ [M + H $^+$]: calculated: 431.1760, found: 431.1758.

3-(3-Hydroxy-3-methylbut-1-yn-1-yl)-8-methyl-4-(phenyl)-2-(quinolin-8-yl)-1,2-dihydroisoquinolin-1-one (4bb).



M.P.: 208–210 °C; Appearance: brown crystal; HPLC yield: 43%; ^1H NMR (400 MHz, Methanol- d_4 , δ 3.31) δ 8.84 (s, 1H), 8.47 (dd, J = 8.3, 2.8 Hz, 1H), 8.12 (dd, J = 8.2, 2.7 Hz, 1H), 7.84 (dd, J = 7.6, 2.5 Hz, 1H), 7.78 (dd, J = 7.9, 2.9 Hz, 1H), 7.64–7.56 (m, 1H), 7.52–7.44 (m, 4H), 7.45–7.39 (m, 2H), 7.34 (s, 1H), 7.17 (dd, J = 8.3, 2.8 Hz, 1H), 2.85 (s, 3H), 0.64 (s, 3H), 0.60 (s, 3H). ^{13}C NMR (101 MHz, Methanol- d_4 , δ 49.00) δ 164.8, 151.9, 145.7, 143.3, 140.4, 138.9, 138.4, 137.9, 133.1, 132.2, 132.1, 131.9, 131., 130.55, 129.5, 129.4, 128.9, 127.8, 126.5, 126.0, 125.7, 125.4, 123.1, 105.5, 76.7, 64.9, 30.4, 24.4. FTIR (cm^{-1}): 3440, 2980, 2120, 1675, 775. HRMS $\text{C}_{30}\text{H}_{24}\text{N}_2\text{O}_2$ [M + H $^+$]: calculated: 445.1916, found: 445.1918.

6-*tert*-Butyl-3-(3-hydroxy-3-methylbut-1-yn-1-yl)-4-phenyl-2-(quinolin-8-yl)-1,2-dihydroisoquinolin-1-one (4cb).

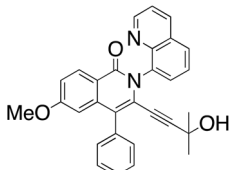


M.P.: 136–138 °C; Appearance: white powder; HPLC yield: 47%; ^1H NMR (400 MHz, Methanol- d_4 , δ 3.31) δ 8.83 (dd, J = 4.3, 1.7 Hz, 1H), 8.48 (dd, J = 8.4, 1.7 Hz, 1H), 8.36 (dd, J = 8.5,



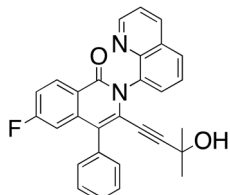
0.5 Hz, 1H), 8.14 (dd, J = 8.2, 1.5 Hz, 1H), 7.86 (dd, J = 7.3, 1.5 Hz, 1H), 7.78 (dd, J = 8.2, 7.4 Hz, 1H), 7.73 (dd, J = 8.5, 1.9 Hz, 1H), 7.60 (dd, J = 8.3, 4.3 Hz, 1H), 7.55–7.43 (m, 5H), 7.41 (dd, J = 1.9, 0.6 Hz, 1H), 1.28 (s, 9H), 0.66 (s, 3H), 0.61 (s, 3H). ^{13}C NMR (101 MHz, Methanol-*d*₄, δ 49.00) δ 164.0, 157.9, 152.0, 145.6, 138.5, 138.4, 137.2, 132.2, 132.0, 131.8, 130.9, 130.7, 129.4, 129.1, 128.7, 127.7, 127.0, 126.9, 126.0, 125.0, 123.1, 123.1, 105.6, 76.8, 64.9, 36.2, 31.3, 30.3. FTIR (cm⁻¹): 3412, 2966, 2120, 1634, 1606, 1567, 1497, 1321, 775. HRMS C₃₃H₃₀N₂O₂ [M + H⁺]: calculated: 487.2386, found: 487.2394.

3-(3-Hydroxy-3-methylbut-1-yn-1-yl)-6-methoxy-4-phenyl-2-(quinolin-8-yl)-1,2-dihydroisoquinolin-1-one (4db).



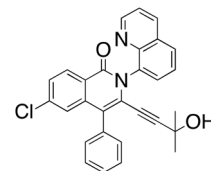
M.P.: 155–156 °C; Appearance: pale yellow crystal; HPLC yield: 56%; ^1H NMR (400 MHz, Methanol-*d*₄, δ 3.31) δ 8.84 (dd, J = 4.3, 1.7 Hz, 1H), 8.48 (dd, J = 8.3, 1.7 Hz, 1H), 8.35 (d, J = 8.9 Hz, 1H), 8.13 (dd, J = 8.2, 1.5 Hz, 1H), 7.85 (dd, J = 7.3, 1.5 Hz, 1H), 7.78 (dd, J = 8.2, 7.3 Hz, 1H), 7.60 (dd, J = 8.4, 4.3 Hz, 1H), 7.57–7.40 (m, 5H), 7.20 (dd, J = 8.9, 2.5 Hz, 1H), 6.75 (d, J = 2.5 Hz, 1H), 3.77 (s, 3H), 0.65 (s, 3H), 0.60 (s, 3H). ^{13}C NMR (101 MHz, Methanol-*d*₄, δ 49.00) δ 164.9, 163.9, 152.0, 145.6, 140.8, 138.5, 138.4, 137.2, 132.2, 132.0, 131.9, 131.0, 130.9, 130.7, 129.5, 129.5, 129.1, 127.7, 126.6, 126.3, 123.1, 120.9, 117.7, 108.5, 105.7, 76.7, 64.9, 55.9, 30.3. FTIR (cm⁻¹): 3320, 2970, 2120, 1760, 1680, 1590, 1230, 1030. HRMS C₃₀H₂₄N₂O₃ [M + H⁺]: calculated: 461.1865, found: 461.1876.

6-Fluoro-3-(3-hydroxy-3-methylbut-1-yn-1-yl)-4-phenyl-2-(quinolin-8-yl)-1,2-dihydroisoquinolin-1-one (4eb).



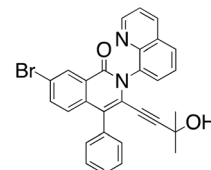
M.P.: 218–220 °C; Appearance: light yellow solid; HPLC yield: 22%; ^1H NMR (400 MHz, CDCl₃, δ 7.26) δ 8.94 (dd, J = 4.4, 1.7 Hz, 1H), 8.55 (dd, J = 8.8, 5.9 Hz, 1H), 8.27 (dd, J = 8.3, 1.7 Hz, 1H), 7.98 (dd, J = 8.3, 1.4 Hz, 1H), 7.83 (dd, J = 7.4, 1.4 Hz, 1H), 7.69 (t, J = 7.8 Hz, 1H), 7.52 (m, 1H), 7.45 (m, 4H), 7.22 (td, J = 8.5, 2.6 Hz, 1H), 7.01 (dd, J = 10.3, 2.5 Hz, 1H), 0.73 (s, 3H), 0.69 (s, 3H). ^{13}C NMR (101 MHz, CDCl₃, δ 77.16) δ 165.6 (d, J = 252.3 Hz), 161.6, 151.1, 144.6, 139.7 (d, J = 10.0 Hz), 137.6, 136.4, 135.6, 131.9 (d, J = 10.0 Hz), 131.3, 130.9, 130.4, 129.3, 129.2, 128.5, 128.4, 128.2, 126.3, 126.2, 123.8 (d, J = 3.1 Hz), 123.2 (d, J = 1.9 Hz), 121.8, 116.0 (d, J = 23.5 Hz), 111.1 (d, J = 23.5 Hz), 103.7, 76.6, 64.8, 29.9. FTIR (cm⁻¹): 3180, 2124, 1655, 1609, 1599, 1469, 1328, 775. HRMS C₂₉H₂₁FN₂O₃ [M + H⁺]: calculated: 449.1665, found: 449.1664.

6-Chloro-3-(3-hydroxy-3-methylbut-1-yn-1-yl)-4-phenyl-2-(quinolin-8-yl)-1,2-dihydroisoquinolin-1-one (4fb).



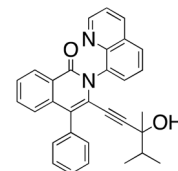
M.P.: 250–252 °C; Appearance: white crystal; HPLC yield: 21%; ^1H NMR (400 MHz, DMSO-*d*₆, δ 2.50) δ 8.88 (dd, J = 4.2, 1.7 Hz, 1H), 8.51 (dd, J = 8.4, 1.7 Hz, 1H), 8.31 (dd, J = 8.5, 0.4 Hz, 1H), 8.16 (dd, J = 8.3, 1.4 Hz, 1H), 7.89 (dd, J = 7.3, 1.4 Hz, 1H), 7.76 (dd, J = 8.2, 7.3 Hz, 1H), 7.66 (dd, J = 8.6, 2.1 Hz, 1H), 7.60 (dd, J = 8.3, 4.2 Hz, 1H), 7.55–7.41 (m, 5H), 7.21 (dd, J = 2.1, 0.5 Hz, 1H), 4.80 (s, 1H), 0.53 (s, 3H), 0.51 (s, 3H). ^{13}C NMR (101 MHz, DMSO-*d*₆, δ 39.52) δ 160.3, 150.9, 143.9, 138.0, 137.9, 137.0, 136.3, 134.6, 130.8, 130.8, 130.1, 130.1, 129.2, 128.7, 128.5, 128.1, 127.7, 126.7, 126.2, 124.3, 124.0, 121.9, 121.2, 106.0, 74.7, 62.8, 30.0. FTIR (cm⁻¹): 3427, 2120, 1634, 1592, 1469, 1321, 775. HRMS C₂₉H₂₁ClN₂O₃ [M + H⁺]: calculated: 465.1370, found: 465.1362.

7-Bromo-3-(3-hydroxy-3-methylbut-1-yn-1-yl)-4-phenyl-2-(quinolin-8-yl)-1,2-dihydroisoquinolin-1-one (4gb).



M.P.: 130–132 °C; Appearance: light brown solid; HPLC yield: 18%; ^1H NMR (400 MHz, Methanol-*d*₄, δ 3.31) δ 8.84 (dd, J = 4.3, 1.7 Hz, 1H), 8.53 (d, J = 2.1 Hz, 1H), 8.49 (dd, J = 8.4, 1.7 Hz, 1H), 8.15 (dd, J = 8.2, 1.5 Hz, 1H), 7.90–7.86 (m, 1H), 7.84 (dd, J = 8.8, 2.2 Hz, 1H), 7.79 (dd, J = 8.2, 7.4 Hz, 1H), 7.61 (dd, J = 8.3, 4.3 Hz, 1H), 7.52–7.43 (m, 5H), 7.30 (d, J = 8.8 Hz, 1H), 0.65 (s, 3H), 0.61 (s, 3H). ^{13}C NMR (101 MHz, Methanol-*d*₄, δ 49.00) δ 162.9, 152.0, 145.4, 138.5, 138.2, 137.4, 137.1, 136.7, 132.1, 132.0, 131.8, 131.3, 131.0, 130.9, 129.6, 129.6, 129.3, 129.0, 128.7, 127.8, 126.7, 126.0, 123.2, 122.6, 106.3, 76.5, 64.9, 30.3. FTIR (cm⁻¹): 3314.54, 2975.90, 2117.84, 1704.07, 1654.71, 1584.12, 1319.06, 1171.12, 789.85. HRMS C₂₉H₂₁BrN₂O₃ [M + H⁺]: calculated: 509.0865, found: 509.0869.

3-(3-Hydroxy-3,4-dimethylpent-1-yn-1-yl)-4-phenyl-2-(quinolin-8-yl)-1,2-dihydroisoquinolin-1-one (5ac).

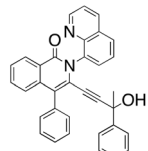


M.P.: 90–94 °C; Appearance: Brown solid; HPLC yield: 32%; ^1H NMR (400 MHz, CDCl₃, δ 7.26) δ 8.90 (dt, 1H), 8.55 (dd, 1H), 8.21 (dt, 1H), 7.94 (dd, 1H), 7.82 (dt, 1H), 7.66 (ddd, 1H), 7.61 (ddd, 1H), 7.53 (m, 2H), 7.43 (m, 5H), 7.36 (m, 1H), 1.13 (hept,



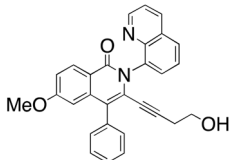
1H), 0.58 (m, 3H), 0.24 (m, 6H). ^{13}C NMR (101 MHz, CDCl_3 , δ 77.16) δ 162.2, 151.1, 144.8, 137.2, 136.3, 136.1, 132.6, 131.4, 131.0, 130.2, 129.3, 129.1, 128.6, 128.4, 128.3, 127.9, 127.5, 126.5, 126.2, 125.7, 125.0, 124.5, 121.7, 101.6, 78.8, 71.5, 38.0, 26.1, 17.2, 16.6. FTIR (cm^{-1}): 3293.77, 2972.55, 2108.37, 1759.30, 1635.63, 1500.25, 1336.25, 1067.30, 726.11. HRMS $\text{C}_{31}\text{H}_{26}\text{N}_2\text{O}_2$ [$\text{M} + \text{H}^+$]: calculated: 459.2073, found: 459.2072.

3-(3-Hydroxy-3-phenylbut-1-yn-1-yl)-4-phenyl-2-(quinolin-8-yl)-1,2-dihydroisoquinolin-1-one (6ad).



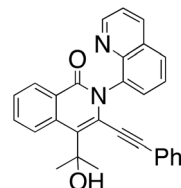
M.P.: 65–70 °C; Appearance: Yellow solid; HPLC yield: 29%; ^1H NMR (400 MHz, CDCl_3 , δ 7.26) δ 8.91 (ddd, $J = 5.9, 4.2, 1.7$ Hz, 1H), 8.56 (ddt, $J = 7.9, 1.5, 0.6$ Hz, 1H), 8.22 (m, 1H), 7.95 (td, $J = 8.1, 1.4$ Hz, 1H), 7.86 (dd, $J = 7.3, 1.4$ Hz, 1H), 7.67 (ddd, $J = 8.2, 7.4, 2.5$ Hz, 1H), 7.63 (tt, $J = 6.8, 1.3$ Hz, 1H), 7.55 (m, 2H), 7.46 (m, 5H), 7.38 (dtd, $J = 8.1, 1.2, 0.6$ Hz, 1H), 7.12 (m, 1H), 7.03 (m, 2H), 6.67 (m, 2H), 0.94 (m, 3H). ^{13}C NMR (101 MHz, CDCl_3 , δ 77.16) δ 162.3, 151.2, 144.9, 144.0, 137.9, 137.2, 136.2, 136.2, 132.7, 131.5, 131.1, 130.3, 129.3, 129.2, 128.7, 128.5, 128.5, 128.1, 128.0, 127.7, 127.6, 126.7, 126.3, 125.9, 124.9, 124.8, 124.5, 121.8, 101.5, 79.8, 69.8, 31.9. FTIR (cm^{-1}): 3321.05, 2981.11, 2113.44, 1765.54, 1647.48, 1489.99, 1369.79, 1044.82, 752.49. HRMS $\text{C}_{31}\text{H}_{26}\text{N}_2\text{O}_2$ [$\text{M} + \text{H}^+$]: calculated: 493.1916, found: 493.1918.

3-(4-Hydroxybut-1-yn-1-yl)-6-methoxy-4-phenyl-2-(quinolin-8-yl)-1,2-dihydroisoquinolin-1-one (7).



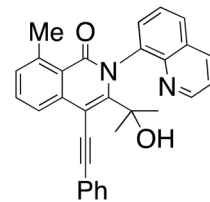
M.P.: 185–186 °C; Appearance: brown sticky solid; Isolated yield: 9%; ^1H NMR (400 MHz, Methanol- d_4) δ 8.83 (dd, $J = 4.3, 1.7$ Hz, 1H), 8.48 (dd, $J = 8.4, 1.7$ Hz, 1H), 8.33 (d, $J = 8.9$ Hz, 1H), 8.13 (dd, $J = 8.2, 1.5$ Hz, 1H), 7.87–7.82 (m, 2H), 7.80–7.74 (m, 1H), 7.63–7.57 (m, 1H), 7.52–7.42 (m, 5H), 7.18 (dd, $J = 8.9, 2.5$ Hz, 1H), 6.98 (d, $J = 8.8$ Hz, 1H), 6.71 (d, $J = 2.5$ Hz, 1H), 3.76 (s, 3H), 2.68 (t, $J = 7.3$ Hz, 2H), 1.78 (t, $J = 7.5$ Hz, 2H). ^{13}C NMR (101 MHz, Methanol- d_4) δ 164.9, 152.0, 145.6, 141.0, 138.6, 138.4, 137.5, 132.2, 132.0, 131.9, 131.0, 130.9, 130.7, 129.6, 129.5, 129.1, 127.7, 127.1, 125.8, 123.2, 120.8, 117.6, 108.4, 99.4, 76.9, 60.6, 55.9, 23.5. FTIR (cm^{-1}): 772, 1252, 1377, 1486, 1603, 1654, 1705, 2928, 3356. HRMS $\text{C}_{29}\text{H}_{22}\text{N}_2\text{O}_3$ [$\text{M} + \text{H}^+$]: calculated: 447.1709, found: 447.1699.

4-(2-Hydroxypropan-2-yl)-3-(2-phenylethynyl)-2-(quinolin-8-yl)-1,2-dihydroisoquinolin-1-one (8).



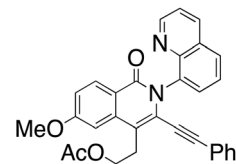
M.P.: 205 °C; Appearance: white sticky solid; Isolated yield: 3%; ^1H NMR (400 MHz, Chloroform- d) δ 8.77 (d, $J = 4.2$ Hz, 1H), 8.48 (d, $J = 8.0$ Hz, 1H), 8.21 (d, $J = 8.3$ Hz, 1H), 8.04 (d, $J = 8.2$ Hz, 1H), 7.78 (d, $J = 7.2$ Hz, 1H), 7.71 (d, $J = 8.3$ Hz, 1H), 7.67 (d, $J = 8.1$ Hz, 1H), 7.62 (d, $J = 8.1$ Hz, 1H), 7.48 (t, $J = 7.6$ Hz, 1H), 7.35 (dd, $J = 8.4, 4.2$ Hz, 1H), 7.03 (d, $J = 6.9$ Hz, 4H), 6.95–6.89 (m, 1H), 3.84 (s, 1H), 1.84 (s, 6H). ^{13}C NMR (101 MHz, Chloroform- d) δ 162.3, 150.6, 143.7, 135.1, 134.8, 134.5, 131.9, 130.9, 129.3, 129.1, 128.7, 128.2, 127.0, 126.9, 126.1, 125.3, 125.1, 124.5, 122.7, 121.4, 121.0, 100.4, 86.4, 76.2, 26.9, 26.8. FTIR (cm^{-1}): 2971.55, 2123.88, 1730, 1459, 1257.79, 1085.05, 788.896. HRMS $\text{C}_{29}\text{H}_{22}\text{N}_2\text{O}_2$ [$\text{M} + \text{H}^+$]: calculated: 431.1760, found: 431.1768.

3-(2-Hydroxypropan-2-yl)-8-methyl-4-(2-phenylethynyl)-2-(quinolin-8-yl)-1,2-dihydroisoquinolin-1-one (9).



M.P.: 212 °C; Appearance: Light Brown; Isolated yield: 2.0%; ^1H NMR (400 MHz, Chloroform- d) δ 8.82 (s, 0H), 8.49 (dd, $J = 9.1, 4.0$ Hz, 0H), 8.17 (d, $J = 8.3$ Hz, 0H), 7.89 (t, $J = 5.3$ Hz, 0H), 7.71 (t, $J = 5.6$ Hz, 0H), 7.63 (d, $J = 8.8$ Hz, 1H), 7.47 (s, 1H), 7.35 (s, 1H), 7.25–7.16 (m, 1H), 7.09 (d, $J = 7.5$ Hz, 0H), 7.02 (d, $J = 8.8$ Hz, 1H), 6.43 (t, $J = 5.8$ Hz, 1H), 5.46 (s, 0H), 3.60 (s, 2H), 2.81 (d, $J = 4.0$ Hz, 1H), 2.58 (s, 0H), 2.12 (d, $J = 4.0$ Hz, 3H), 2.00–1.92 (m, 3H), 1.82 (s, 1H), 1.19 (s, 4H), 0.80 (d, $J = 9.8$ Hz, 1H). ^{13}C NMR (101 MHz, Chloroform- d) δ 162.8, 151.1, 142.4, 139.0, 137.7, 136.1, 130.6, 130.5, 129.2, 128.8, 128.6, 128.1, 127.9, 126.4, 126.0, 123.2, 121.7, 102.6, 85.4, 74.3, 32.0, 24.8. FTIR (cm^{-1}): 3440, 2980, 2120, 1675, 775. HRMS $\text{C}_{29}\text{H}_{22}\text{N}_2\text{O}_2$ [$\text{M} + \text{Na}^+$]: calculated: 467.1735, found: 467.1724.

2-[6-Methoxy-1-oxo-3-(2-phenylethynyl)-2-(quinolin-8-yl)-1,2-dihydroisoquinolin-4-yl]ethyl acetate (10).

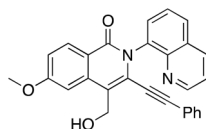


M.P.: 172–173 °C; Appearance: off-white solid; HPLC based yield: 9.3%; Isolated yield: 8.0 mg (4.3%); ^1H NMR (400 MHz, CDCl_3 , TMS) δ 8.81 (dd, $J = 4.0, 2.0$ Hz, 1H), 8.39 (dd, $J = 8.8$,



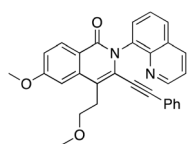
1.5 Hz, 1H), 8.18 (d, J = 8.2 Hz, 1H), 7.93 (d, J = 8.1 Hz, 1H), 7.75 (d, J = 7.3 Hz, 1H), 7.64 (t, J = 7.6 Hz, 1H), 7.34 (dd, J = 8.6, 4.0 Hz, 1H), 7.28 (t, J = 2.0 Hz, 7H), 7.13 (m, 2H), 7.06 (m, 3H), 6.62 (m, 2H), 4.35 (m, 2H), 3.95 (s, 3H), 3.33 (t, J = 7.9 Hz, 2H), 1.97 (s, 3H). ^{13}C NMR (101 MHz, CDCl_3 , TMS) δ 170.2, 162.3, 160.8, 150.1, 143.9, 137.4, 137.0, 135.0, 130.10, 130.0, 129.2, 128.1, 128.1, 127.8, 127.1, 125.9, 125.1, 120.6, 119.5, 115.5, 115.2, 104.4, 98.4, 81.9, 61.9, 54.7, 28.2, 20.0. FTIR (cm^{-1}): 3321.42, 2844.40, 1734.40, 1605.65, 1336.63, 1022.75, 795.952. MALDI $\text{C}_{31}\text{H}_{24}\text{N}_2\text{O}_4$ [M + H $^+$]: calculated: 489.18, found: 489.18.

4-(Hydroxymethyl)-6-methoxy-3-(2-phenylethynyl)-2-(quinolin-8-yl)isoquinolin-1-one (13).



M.P.: 211–212 °C. **Appearance:** white solid; **Isolated yield:** 56 mg (51%); ^1H NMR (400 MHz, CDCl_3) δ 8.85 (dd, J = 4.3, 1.7 Hz, 1H), 8.42 (d, J = 8.9 Hz, 1H), 8.22 (dd, J = 8.3, 1.7 Hz, 1H), 7.98 (dd, J = 8.2, 1.4 Hz, 1H), 7.82 (dd, J = 7.3, 1.4 Hz, 1H), 7.69 (t, J = 7.8 Hz, 1H), 7.41 (d, J = 2.4 Hz, 1H), 7.38 (dd, J = 8.3, 4.2 Hz, 1H), 7.22–7.15 (m, 1H), 7.11 (dd, J = 8.9, 2.4 Hz, 1H), 7.09 (t, J = 7.6 Hz, 2H), 6.63 (dd, J = 8.3, 1.3 Hz, 2H), 5.11 (s, 2H), 3.97 (s, 3H), 2.40 (s, 1H). ^{13}C NMR (101 MHz, CDCl_3) δ 163.4, 162.2, 151.3, 144.9, 138.2, 137.9, 136.2, 131.1, 130.8, 130.5, 129.2, 129.2, 129.1, 128.2, 127.4, 126.3, 121.8, 121.3, 120.6, 119.7, 116.8, 106.0, 99.9, 82.4, 60.8, 55.7. FTIR (cm^{-1}): 3414, 3059, 2107, 1654, 1605, 1492, 1250, 1207, 795. HRMS: $\text{C}_{28}\text{H}_{20}\text{N}_2\text{O}_3$ [M + H $^+$]: calculated 433.1552, found: 433.1555.

6-Methoxy-4-(2-methoxyethyl)-3-(2-phenylethynyl)-2-(quinolin-8-yl)-1,2-dihydroisoquinolin-1-one (14).



M.P.: 215–216 °C; **Appearance:** white solid; **Isolated yield:** 84 mg (56%); ^1H NMR (400 MHz, Chloroform- d) δ 8.80 (dd, J = 4.2, 1.7 Hz, 1H), 8.39 (d, J = 8.8 Hz, 1H), 8.16 (dd, J = 8.4, 1.7 Hz, 1H), 7.91 (dd, J = 8.3, 1.4 Hz, 1H), 7.74 (dd, J = 7.3, 1.4 Hz, 1H), 7.62 (dd, J = 8.2, 7.3 Hz, 1H), 7.31 (dd, J = 8.3, 4.2 Hz, 1H), 7.19–7.15 (m, 1H), 7.10 (d, J = 7.4 Hz, 1H), 7.07–7.01 (m, 3H), 6.64–6.57 (m, 2H), 3.89 (s, 3H), 3.69–3.62 (m, 2H), 3.35 (s, 3H). ^{13}C NMR (101 MHz, CDCl_3) δ 163.2, 161.8, 151.2, 144.9, 138.7, 138.1, 136.0, 131.1, 130.9, 130.2, 129.1, 129.0, 128.8, 128.2, 126.6, 126.1, 121.6, 121.6, 120.6, 117.7, 115.8, 105.8, 99.5, 83.1, 71.8, 58.8, 55.6, 30.1. FTIR (cm^{-1}): 3044, 2866, 2113, 1645, 1599, 1238, 1106, 751. HRMS: $\text{C}_{30}\text{H}_{24}\text{N}_2\text{O}_3$ [M + H $^+$]: calculated 461.1865, found: 461.1864.

Author contributions

PD and PA performed the syntheses and analyses. IAN and SK conceived the project. JW undertook the NMR studies. All authors contributed to the writing of the manuscript and gave approval for submission.

Conflicts of interest

There are no conflicts of interest to declare.

Acknowledgements

We thank Linnaeus University, the Swedish Research Council (Vetenskapsrådet, grant number 2014-4573), and the Swedish Knowledge Foundation (grant number 20190114) for financial support. We are grateful to Dr Subramanian Suriyanarayanan (LNU) and Prof. Kothandaraman Ramanjuam (IIT-Madras, Chennai) for help with XRD studies.

References

- 1 T. Dalton, T. Faber and F. Glorius, *ACS Cent. Sci.*, 2021, **7**, 245–261.
- 2 R. H. Crabtree, *J. Organomet. Chem.*, 2004, **689**, 4083–4091.
- 3 M. Zhang, Y. Zhang, X. Jie, H. Zhao, G. Li and W. Su, *Org. Chem. Front.*, 2014, **1**, 843–895.
- 4 Z. Chen, B. Wang, J. Zhang, W. Yu, Z. Liu and Y. Zhang, *Org. Chem. Front.*, 2015, **2**, 1107–1295.
- 5 M. Moselage, J. Li and L. Ackermann, *ACS Catal.*, 2016, **6**, 498–525.
- 6 O. Daugulis, H.-Q. Do and D. Shabashov, *Acc. Chem. Res.*, 2009, **42**, 1074–1086.
- 7 T. K. Hyster and T. Rovis, *J. Am. Chem. Soc.*, 2010, **132**, 10565–10569.
- 8 J. M. Neely and T. Rovis, *J. Am. Chem. Soc.*, 2013, **135**, 66–69.
- 9 H. Wang, C. Grohmann, C. Nimpfius and F. Glorius, *J. Am. Chem. Soc.*, 2012, **134**, 19592–19595.
- 10 L. Ackermann, *Acc. Chem. Res.*, 2014, **47**, 281–295.
- 11 K. Padala and M. Jeganmohan, *Org. Lett.*, 2011, **13**, 6144–6147.
- 12 P. B. Arockiam, C. Bruneau and P. H. Dixneuf, *Chem. Rev.*, 2012, **112**, 5879–5918.
- 13 X. Li, W. Ouyang, J. Nie, S. Ji, Q. Chen and Y. Huo, *ChemCatChem*, 2020, **12**, 2358–2384.
- 14 P. Gandeepan, T. Müller, D. Zell, G. Cera, S. Warratz and L. Ackermann, *Chem. Rev.*, 2019, **119**, 2192–2452.
- 15 K. Gao and N. Yoshikai, *Acc. Chem. Res.*, 2014, **47**, 1208–1219.
- 16 D. Wei, X. Zhu, J.-L. Niu and M.-P. Song, *ChemCatChem*, 2016, **8**, 1242–1263.
- 17 Y. Kommagalla and N. Chatani, *Coord. Chem. Rev.*, 2017, **350**, 117–135.



18 T. Yoshino and S. Matsunaga, *Asian J. Org. Chem.*, 2018, **7**, 1193–1205.

19 H. Zhang, M.-C. Sun, D. Yang, T. Li, M.-P. Song and J.-L. Niu, *ACS Catal.*, 2022, **12**, 1650–1656.

20 F. H. Lutter, S. Graßl, L. Grokenberger, M. S. Hofmayer, Y.-H. Chen and P. Knochel, *ChemCatChem*, 2019, **11**, 5188–5197.

21 L. Grigorjeva and O. Daugulis, *Org. Lett.*, 2015, **17**, 1204–1207.

22 T. T. Nguyen, L. Grigorjeva and O. Daugulis, *ACS Catal.*, 2016, **6**, 551–554.

23 T. T. Nguyen, L. Grigorjeva and O. Daugulis, *Angew. Chem., Int. Ed.*, 2018, **57**, 1688–1691.

24 D.-G. Yu, T. Gensch, F. de Azambuja, S. Vásquez-Céspedes and F. Glorius, *J. Am. Chem. Soc.*, 2014, **136**, 17722–17725.

25 D. Zhao, J. H. Kim, L. Stegemann, C. A. Strassert and F. Glorius, *Angew. Chem., Int. Ed.*, 2015, **54**, 4508–4511.

26 T. Gensch, F. J. R. Klauck and F. Glorius, *Angew. Chem., Int. Ed.*, 2016, **55**, 11287–11291.

27 A. Lerchen, T. Knecht, M. Koy, C. G. Daniliuc and F. Glorius, *Chem. – Eur. J.*, 2017, **23**, 12149–12152.

28 W. Song and L. Ackermann, *Angew. Chem., Int. Ed.*, 2012, **51**, 8251–8254.

29 N. Sauermann, R. Mei and L. Ackermann, *Angew. Chem., Int. Ed.*, 2018, **57**, 5090–5094.

30 B. V. Pati, P. S. Sagara, A. Ghosh, G. K. Das Adhikari and P. C. Ravikumar, *J. Org. Chem.*, 2021, **86**, 9428–9443.

31 M. Sen, R. Mandal, A. Das, D. Kalsi and B. Sundararaju, *Chem. – Eur. J.*, 2017, **23**, 17454–17457.

32 T. Yoshino and S. Matsunaga, *Adv. Synth. Catal.*, 2017, **359**, 1245–1262.

33 K. Bhadra and G. S. Kumar, *Mini-Rev. Med. Chem.*, 2010, **10**, 1235–1247.

34 M. Bian, L. Ma, M. Wu, L. Wu, H. Gao, W. Yi, C. Zhang and Z. Zhou, *ChemPlusChem*, 2020, **85**, 388–388.

35 T. Bosanac, E. R. Hickey, J. Ginn, M. Kashem, S. Kerr, S. Kugler, X. Li, A. Olague, S. Schlyer and E. R. R. Young, *Bioorg. Med. Chem. Lett.*, 2010, **20**, 3746–3749.

36 Z. Jin, *Nat. Prod. Rep.*, 2013, **30**, 849–868.

37 M. Itoh, M. Shimizu, K. Hirano, T. Satoh and M. Miura, *J. Org. Chem.*, 2013, **78**, 11427–11432.

38 D.-G. Yu, F. de Azambuja, T. Gensch, C. G. Daniliuc and F. Glorius, *Angew. Chem., Int. Ed.*, 2014, **53**, 9650–9654.

39 S. Kathiravan and I. A. Nicholls, *Org. Lett.*, 2017, **19**, 4758–4761.

40 A. Dey and C. M. R. Volla, *Org. Lett.*, 2020, **22**, 7480–7485.

41 S. Kumar, S. Nunewar, T. K. Sabbi and V. Kanchupalli, *Org. Lett.*, 2022, **24**, 3395–3400.

42 R. Mei, W. Ma, Y. Zhang, X. Guo and L. Ackermann, *Org. Lett.*, 2019, **21**, 6534–6538.

43 S. K. Yadav, B. Ramesh and M. Jeganmohan, *J. Org. Chem.*, 2022, **87**, 4134–4153.

44 Y. Luo, H. Liu, J. Zhang, M. Liu and L. Dong, *Org. Lett.*, 2020, **22**, 7604–7608.

45 S. Qian, X. Pu, G. Chang, Y. Huang and Y. Yang, *Org. Lett.*, 2020, **22**, 5309–5313.

46 F. Zhao, X. Gong, Y. Lu, J. Qiao, X. Jia, H. Ni, X. Wu and X. Zhang, *Org. Lett.*, 2021, **23**, 727–733.

